Molecular BioSystems

Accepted Manuscript

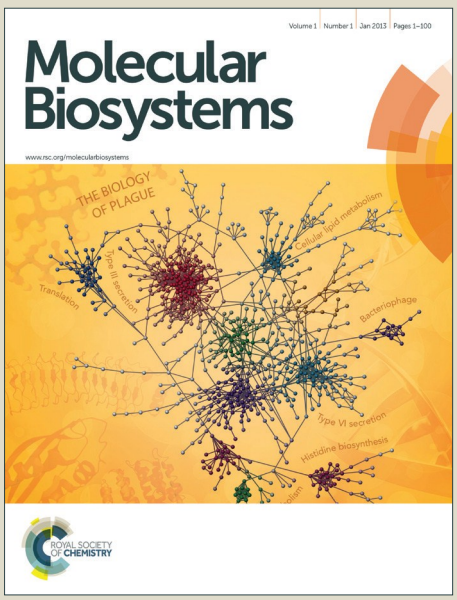

ROYAL SOCIETY OF CHEMISTRY

www.rsc.org/molecularbiosystems

The proteome of methylmalonic acidemia (MMA): elucidation of altered pathways in patient livers

Marianna Caterino[1,2,3#], Randy J. Chandler[4#], Jennifer L. Sloan[4], Kenneth Dorko[5], Kristina Cusmano-Ozog[6], Laura Ingenito[2], Stephen C. Strom[7], Esther Imperlini[2], Emanuela Scolamiero[2], Charles P. Venditti[4]* and Margherita Ruoppolo[1, 2, 3*]

[1]Dipartimento di Medicina Molecolare e Biotecnologie Mediche, Università degli Studi di Napoli, "Federico II", Naples, Italy

[2]CEINGE Biotecnologie Avanzate, Naples, Italy,

[3]Associazione Culturale DiSciMuS RFC 80026 Casoria (NA)

[4]Organic Acid Research Section, Genetics and Molecular Biology Branch, National Human Genome Research Institute, National Institute of Health, Bethesda MD 2092

[5]Department of Pharmacology, Toxicology and Therapeutics, University of Kansas Medical Center, Kansas City, Kansas, USA

[6]Division Genetics and Metabolism, Children's National Medical Center, Washington DC USA

[7]Department of Laboratory Medicine, Division of Pathology, Karolinska Institutet, Stockholm, Sweden

[#] Equal contribution/co-first authors

*Corresponding authors: Margherita Ruoppolo, Dipartimento di Medicina Molecolare e Biotecnologie Mediche, Università degli Studi di Napoli, "Federico II", Via Pansini, 5, 80131 Naples, Italy. Tel: +39-081-7462426; Fax:+39-081-7462417; e-mail: margherita.ruoppolo@unina.it; Charles P. Venditti, Organic Acid Research Section, Genetics

and Molecular Biology Branch, National Human Genome Research Institute, National Institute of Health, Bethesda MD 2092, e-mail: venditti@mail.nih.gov

Word counts: 4273

Number of figures and tables: 7

Abstract

Methylmalonic acidemia (MMA) is a heterogeneous and severe autosomal recessive inborn error of metabolism most commonly caused by the deficient activity of the vitamin B12 dependent enzyme, methylmalonyl-CoA mutase (MUT). The main treatment for MMA patients is dietary restriction of propiogenic amino acids and carnitine supplementation. Despite treatment, the prognosis for vitamin B12 non-responsive patients remains poor and is associated with neonatal lethality, persistent morbidity and decreased life expectancy. While multi-organ pathology is a feature of MMA, the liver is severely impacted by mitochondrial dysfunction which likely underlies the metabolic instability experienced by the patients. Liver and/or combined liver/kidney transplantation are therefore sometimes performed in severely affected patients. Using liver specimens from donors and MMA patients undergoing elective liver transplantation collected under a dedicated natural history protocol (clinicaltrials.gov: NCT00078078), we employed proteomics to characterize the liver pathology and impaired hepatic metabolism observed in the patients. Pathway analysis revealed perturbations of enzymes involved in energy metabolism, gluconeogenesis and Krebs cycle anaplerosis. Our findings identify new pathophysiologic and therapeutic targets that could be valuable for designing alternative therapies to alleviate clinical manifestations seen in this disorder.

Abbreviations:

ALDOB, Aldolase B; ASS1, argininosuccinate synthetase 1; AKR1A1, aldo-ketoreductase family 1, member A1; CA1, carbonic anhydrase 1; CATSD, cathepsin D; CPS1, carbamoyl-phosphate synthase 1; DIGE (Differential Gel Electrophoresis); GI, gene ID GLUD2, glutamate dehydrogenase 2; HMGCS2, HMGCS2 3-hydroxy-3-methylglutaryl-CoA synthase 2; MUT, methylmalonyl-CoA mutase; MMA, isolated methylmalonic acidemia; MS, mass spectrometry; PCK2, phosphoenlopyruvate carboxykinase 2; PYGL, glycogen phosphorylase;

SDH, succinate dehydrogenase; TPI1, triosephosphate isomerase 1; TRAP1, TNF receptor-associated protein 1; UROC1, urocanase domain containing

Concise sentence

Proteome profile of hepatic tissue isolated from methylmalonic acidemia (MMA) patients reveals deregulation in protein expression of enzymes involved in energy metabolism, gluconeogenesis and Krebs cycle anaplerosis.

Compliance with Ethics Guidelines

All authors have contributed to, and read, the paper and have given permission for their name to be included as a co-author. The manuscript, including figures and tables, has not been previously published and is not under consideration elsewhere.

Conflict of Interest:

Marianna Caterino declares that she has no conflict of interest. Randy J. Chandler declares that she has no conflict of interest. Jennifer L. Sloan declares that she has no conflict of interest. Kenneth Dorko declares that she has no conflict of interest. Kristina Cusmano-Ozog declares that she has no conflict of interest. Laura Ingenito declares that she has no conflict of interest. Stephen C. Strom declares that she has no conflict of interest. Esther Imperlini declares that she has no conflict of interest. Emanuela Scolamiero declares that he has no conflict of interest. Charles P. Venditti declares that he has no conflict of interest.

Margherita Ruoppolo declares that she has no conflict of interest.

Informed Consent

All procedures followed were in accordance with the ethical standards of the responsible committee on human experimentation (institutional and national) and with the Helsinki Declaration of 1975, as revised in 2000. Informed consent was obtained from all patients for being included in the study.

Introduction

Methylmalonic acidemia (MMA) is one of the most common inborn errors of organic acid metabolism and is usually caused by the deficient activity of mitochondrial adenosylcobalamin-dependent methylmalonyl-CoA mutase (MUT, EC 5.4.99.2). MUT converts L-methylmalonyl-CoA into succinyl-CoA, a Krebs cycle intermediate. This reaction is essential for the metabolism of propionyl-CoA, an important intermediate in the degradation of isoleucine, valine and odd-chain fatty acids. A block at this enzymatic step results in elevated plasma levels of methylmalonic acid as well the accumulation of other propionyl-CoA-derived metabolites such as 2-methylcitrate[1].

The main treatment for vitamin B12 non-responsive patients is through the dietary restriction of propiogenic amino acids, especially isoleucine and valine, to reduce circulating metabolites[2-4]. Patients with mutations in the *MUT* gene typically have severe disease and demonstrate poor outcomes, with early mortality and substantial lifelong morbidity[5-7]. They exhibit multisystemic manifestations, such as "metabolic strokes" of the basal ganglia[8.9], a propensity to develop pancreatitis[10], progressive renal insufficiency[11], and a perhaps most importantly, a predisposition to develop metabolic crises in the face of stress, dietary indiscretion and/or infection.

Liver[12-14] kidney[15] and/or combined liver/kidney[16,17] transplantation has been performed in a limited fashion in an attempt to improve metabolic stability through the provision of organ-specific enzymatic activity. The pathophysiology of disease manifestations in MMA remains unknown. Although the MUT enzyme is expressed ubiquitously, it is not present at the same levels in all tissues[18] and the clinical features observed in the patients indicate a tissue-specific vulnerability[19,20]. Because patients that have received liver transplantations are effectively cured of the propensity to develop recurrent metabolic instability, we have used liver specimens from donors and MMA patients that received elective liver or combined liver-

kidney transplantation to identify deregulated proteins using differential proteomics. The pathways perturbed by the underlying disease represent targets for the design of therapies to alleviate clinical manifestations of the disorder, and delineate the hepatic adaptations that occur in patients with MMA.

Experimental Section

Patient and control livers

MMA patient livers were obtained in compliance with the Helsinki Declaration and were approved by the National Human Genome Research Institute Institutional Review Board as part of NIH study 04-HG-0127 "Clinical and Basic Investigations of Methylmalonic Acidemia and Related Disorders" (clinicaltrials.gov: NCT00078078). The patient materials were derived from the discarded livers from patients undergoing either elective liver or combined liver/kidney transplant procedures. Because the livers from patients with MMA are not suitable for transplantation, they were considered surgical waste specimens and subsequently procured from the operating room for research use. The liver tissues were snap frozen in liquid nitrogen and then held at -80°C until use. In all cases, the diagnosis was vitamin B12 non-responsive MMA. Cellular biochemical studies, including [1-^{14}C] propionate incorporation studies on skin fibroblasts, molecular genetics and clinical metabolic parameters, such as massive elevations of methylmalonic acid and related propionyl-CoA derived metabolites, indicated a vitamin B12 non-responsive form of MMA (Table 1). Control liver samples were procured from adults who had undergone liver resection, typically after trauma (Table 1), and then donated their liver tissues to the University of Pittsburgh cell isolation facility (Pittsburgh, PA, USA), established as part of an NIH-funded liver tissue cell distribution system. The collection of resected liver specimens was approved by the University of Pittsburgh Institutional Review Board (IRB Number 0411142).

In all cases, the livers were obtained from the operating room while the donor was alive or well perfused, and either snap frozen in liquid nitrogen in the case of MMA patients in the operating room, or processed in an identical fashion in a hepatocyte isolation facility (controls) and proven to yield hepatocytes in high viability before further study.

Metabolite studies

Frozen wedges of liver (400mg) were homogenized in 1 ml of 4% perchloric acid by using Dounce tissue homogenizer. The mechanical disruption of human tissues was obtained by using a loose pestle. After centrifugation to remove proteins, supernatant were adjusted to pH 6-7 with KOH and re-centrifuged. Amino acids, acylcarnitines and organic acids were measured in the resulting supernatant. The protein pellet was dissolved in 1M NaOH and results were normalized to protein as determined by Lowry assay.

Amino acids and acylcarnitines were measured by LC-MS/MS as described[21]. Analysis was performed using an API 2000 triple quadrupole mass spectrometer (Applied Biosystems-Sciex, Toronto, Canada) coupled with the Agilent high performance liquid chromatograph of the 1100 series (Agilent Technologies, Waldbronn, Germany). Data were quantitatively analysed with ChemoView v1.2 software by comparing the signal intensities of the analyte and its corresponding internal standard.

Organic acids were measured using GC/MS as described[21]. GC/MS analysis was carried out with a fused silica capillary column 30 m × 0.25-mm internal diameter, fitted with a fused methyl silicone DB-1 column. The GC/MS system consisted of an Agilent 7890A (Agilent Technologies, Waldbronn, Germany) gas chromatograph and an Agilent 5975C (Agilent Technologies, Waldbronn, Germany) mass spectrometer. After data acquisition, the organic acids were identified using the NIST process and the Wiley mass spectra library (release 2008). Compounds were quantified on the basis of the areas of total ion chromatograms.

Metabolites were quantified by comparing the area of each compound with the area of the internal standards used at known concentrations.

Differential Gel Electrophoresis (DIGE)

DIGE experiments were performed on liver extracts from six MMA patients and six donors as previously described[22-24]. Liver tissues were homogenized in 0.5 ml of lysis buffer (7M urea, 2M thiourea, 4% chaps, 30mM Tris-HCl pH 7.5) using a Dounce homogenizer. The protein extract concentrations were determined and equal amounts of the protein lysates deriving from each control (n=6) and patients (n=6) were then labeled *in vitro* using two different fluorescent cyanine minimal dyes (Cy3 and Cy5, respectively) differing in their excitation and emission wavelengths. A third cyanine dye (Cy2) was used to label a mixture of all samples, controls and patients (n=12) as internal standard. Isoelectric focusing was peformed at a pH range of 3-10 over a length of 24 cm. Six gels were obtained, each of them contained three differently labeled protein mixtures constituted by one patient, one control and the internal standard. The reducing and alkylating steps were performed between the first and the second electrophoretic step.

Acrylamide strips were then transferred to the top of a classical SDS PAGE gel for a second orthogonal electrophoresis analysis. The Cy2, Cy3 and Cy5 images were obtained by scanning each of the six DIGE gels at excitation/emission wavelength of 480/ 530 nm for Cy2, 520/590 nm for Cy3 and 620/680 nm for Cy5 using a Typhoon 9410 TM scanner (GE Healthcare). A semi-preparative gel, prepared in an identical fashion, but obtained by using 500 μg of total protein extract, was scanned with 480/633 nm wavelengths. After consecutive excitation at both wavelengths, the images from the preparative gel were overlaid and subtracted (normalized) from the samples, whereby only differences (up or down regulated proteins) between the two samples were visualized. Images were analyzed using the DeCyder

software suite, version 5.02 (GE Healthcare) in batch processing mode as described previously[22-24]. Each spot intensity was expressed as mean of six standard abundances calculated for the six gels. Spot intensities were then compared in the two conditions under analysis: MMA and control livers. The statistical significance of differences in spot intensity was determined by Student's t-test. Only protein spots with fold changes of at least 1.1 in volume ($p \leq 0.05$) after normalization were considered significantly altered. We verified the accuracy of spot matching by manual investigation.

The gels showed a high degree of similarity, with more than 80% of all spots not showing any variations in the intensity and therefore representing proteins which do not have a different expression in the two conditions (Figure 1S of supplemental materials). The remaining 20% showed variation in the intensity and were further studied because they represents dysregulated proteins in patients.

Proteomic analysis

The spots of interest were excised, hydrolyzed and the peptide mixtures analyzed by mass spectrometry, MALDI-MS and LC-MSMS using respectively 4800 Plus MALDI TOF/TOF™ Analyzer, Applied Biosystems 4800 Proteomics Analyzer (Applied Biosystems, Framingham, MA, USA) and a LC/MSD Trap XCT Ultra (Agilent Technologies, Palo Alto, CA) equipped with a 1100 HPLC system and a chip cube (Agilent Technologies). MALDI spectra were acquired in the positive ion reflector mode using delayed extraction in the mass range between 800 and 4000 Da. LC-MSMS analysis was performed using data-dependent acquisition of one MS scan followed by MS/MS scans of the three most abundant ions in each MS scan. Raw data analyses were converted into a Mascot format text to identify proteins using Matrix Science software. The protein search considered the following parameters: non-redundant protein sequence database (NCBInr), specificity of the proteolytic enzyme used for

the hydrolysis (trypsin), taxonomic category of the sample, no protein molecular weight was considered, up to one missed cleavage, cysteines as S-carbamidomethylcysteines, unmodified N- and C-terminal ends, methionines both unmodified and oxidized, putative pyro-Glu formation by Gln, precursor peptide maximum mass tolerance of 200 ppm, and a maximum fragment mass tolerance of 200 ppm.

Western blot studies

Protein extracts (10 μg) from livers of MMA patients and donors were analyzed by immunoblotting with monoclonal antibodies anti-β-actin (Sigma Aldrich), anti-UROC1 (Santa Cruz, sc-99712, rabbit polyclonal), anti-ASS1 (Santa Cruz, sc-99718, rabbit polyclonal), anti-AKR1A1 (Santa Cruz, sc-100500, mouse monoclonal), anti-HMGCS2 (Santa Cruz, sc-33828, rabbit polyclonal), anti-GLUD2 (Santa Cruz, sc-160382, goat polyclonal). The anti-β-actin was used at 1:5,000 and all monoclonal antibodies were used at a dilution of 1:1000. Immunoblot detections were carried out using HRP-conjugated secondary antibodies and enhanced chemiluminescence (GE Healthcare, Piscataway, NJ). The resulting Western blot images were scanned and analyzed using Chemi Doc software (Biorad, Hercules, CA).

Results

Patient's clinical characteristics

Table 1 presents basic information on the age, sex and enzymatic characterization of the patients with MMA compared to controls. The controls had variably suffered from motor vehicle trauma, cerebrovascular accidents, and intracranial hemorrhages yet were deemed organ donors. Furthermore, lobes from each control were tested for the ability to produce viable hepatocytes in high yield as a criterion for inclusion in this study. All patients with MMA had massive biochemical perturbations and were clinically non-responsive to vitamin B12. Patients M1-M4 had additional cellular characterization and mutation analyses.

Metabolite studies

A combination of LC-MS/MS and GC/MS based metabolic measurements were performed and metabolite concentrations were normalized to the protein content of the extract. As presented in Table 2, propionyl (C3) and methylmalonyl (C4DC) carnitine esters as well as glycine and methylmalonic acid were significantly increased in the liver extracts of the six patients compared to controls, while succinate was decreased.

Differential proteomics

Protein lysates from liver tissue from six MMA patients were used to identify dysregulated proteins compared to liver tissue from six controls. The set of representative fluorescent scans is depicted in Figure 1S of supplemental materials. A quantitative analysis was performed so that only proteins up or down regulated in all six patients versus controls were taken into account. The preparative gel, labeled with proteins that migrated to each spot, is presented in Figure 1.

We identified 19 up- and 37-down regulated proteins in the hepatic proteome of MMA patients compared to controls (Tables 3 and 4). Spot numbers are shown. For each protein, fold change, *p*-value, protein description, GI (sequence identification number provided by NCBI), gene ID, official symbol (sequence identification number provided by HGCN), MW and pI are presented. Details of the mass spectrometric identification, i.e. the identified peptide sequence, the MASCOT score for each peptide and the number of identified peptides for protein, are presented in Table 1S and 2S of supplemental materials.

The whole groups of differentially expressed proteins and metabolites were analysed using the Ingenuity Pathway Analysis (IPA) software 7.0 (http://www.ingenuity.com) to evaluate the significant networks and canonical pathways associated with the 56 proteins differentially expressed and 6 alterated metabolites. The top-ranked network was in Amminoacid Metabolism and Carbohydrate Metabolism with a score of 48, in which 20 nodes out of 35 (57% of the total nodes) were represented by proteins and metabolites identified in this study (Figure 2S of supplemental materials). Many proteins have interaction with insulin, the most important hormone regulating carbohydrate metabolism. Next, the statistically enriched canonical pathways were explored. IPA analysis revealed perturbations in a variety of pathways including small molecule biochemistry, carbohydrate, amino acid and nucleic acid metabolism, free radical scavenging and molecular transport

Western blot analyses of deregulated proteins

Western blot analyses were performed to examine differentially expressed proteins. A major constraint was the availability of commercial antibodies and whether those tested detected the targets as advertised. Figure 2 shows the results of the experiments confirming the relative increased expression of 3-hydroxy-3-methylglutaryl-CoA synthase 2 (HMGCS2, Santa Cruz, sc-33828, rabbit polyclonal), glutamate dehydrogenase 2 (GLUD2, Santa Cruz, sc-160382,

gooat polyclonal) and decreased expression of aldo-ketoreductase family 1, member A1 (AKR1A1, Santa Cruz, sc-100500, mouse monoclonal), urocanase domain containing 1 (UROC1, Santa Cruz, sc-99712, rabbit polyclonal), and argininosuccinate synthetase 1 (ASS1, Santa Cruz, sc-99718, rabbit polyclonal) compared to beta-actin. Western blot analysis was performed in six independent replicates. Optical density was measured for each sample and normalized using beta actin run on the same gel. In Figure 2 B the results are shown as means ± SD.

Discussion

The primary objective of this study was to identify differentially expressed proteins in livers from 6 patients with severe MMA. Although it is well recognized that the 2D-DIGE technique used here only allows for the detection of a small portion of the hepatic proteome in comparison to proteomic methods that utilize LC/MS-MS, we and others have successfully used this method as a starting point to perform comparative proteomics on samples derived from patients with IEMs.

The top-ranked network was in Amminoacid Metabolism and Carbohydrate Metabolism with a score of 48, in which 20 nodes out of 35 (57% of the total nodes) were represented by proteins and metabolites identified in this study (Figure 2S of supplemental materials). Many proteins have interaction with insulin, the most important hormone regulating carbohydrate metabolism. These proteins and metabolites will be further discussed below.

In addition we reported perturbations in pathways including amino acid and nucleic acid metabolism, free radical scavenging and molecular transport. These pathways include a small percentage of proteins identified in this study and need further investigations.

As stated above, most of the differentially abundant proteins detected in our proteomic are involved in metabolic pathways such as energy and carbohydrate metabolism. These include decreased levels of succinate dehydrogenase (SDHA) and ATP synthase (ATP5B); the gluconeogenic enzymes, phosphoenlopyruvate carboxykinase 2 (PCK2), aldolase B (ALDOB), and triosephosphate isomerase1(TPI1) and glycogen phosphorylase (PYGL). Conversely, increased levels of 3-hydroxy-3-methylglutaryl-CoA synthase 2 (HMGS2) and glutamate dehydrogenase (GLUD 1 and 2) (Figure 3) were noted. In total, the pattern of changes may suggest that the MMA liver is attempting a metabolic adaptation, perhaps as a compensation for mitochondrial dysfunction that is well-recognized in mice and patients with MUT deficiency[19,25].

While the pattern of metabolites observed in the patient livers, such as increased methymalonic acid and propionylcarnitine, was expected, the more intriguing observation is the reduction of intermediates of the citric acid cycle, in particular succinate (Table 2). As others have also suggested[26], it would be interesting to investigate whether supplementation of alternative energy substrates such as succinate might be beneficial for metabolic maintenance treatment in patients with MMA. The data reported here provide the first direct measurements to support this approach.

Among the differentially expressed proteins that were upregulated in the MMA patient livers, both 3-hydroxy-3methylglutaryl-CoA synthase 2 and glutamate dehydrogenase 1 and 2 (GLUD1 and 2) may have particular relevance to metabolic adaptations caused by the underlying disorder. The inhibition of citric acid cycle activity due to the lack of intermediates, oxaloacetate, succinate and malate facilitate the formation of ketone bodies from acetyl CoA and perhaps increased levels of 3-hydroxy-3-methylglutaryl-Coa synthase 2 (HMGS2) may contribute to the propensity of patients with MMA to develop ketonemia/ketonuria. Similarly, ureagenesis is disturbed in MMA and manifests as a propensity to develop hyperammonemia in the patients; the reasons are unclear and likely multifactorial. One theory posits that the functional lack of β-ketoglutarate due to an impairment of Krebs cycle in MMA could shift the equilibrium of the reaction catalyzed by glutamate dehydrogenase, producing ammonia and consuming hepatic glutamate stores. The subsequent observations[27] showing that hyperammonemia in patients with propionic acidemia was accompanied by a decrease of the plasma levels of glutamine/glutamate support this theory. It is therefore intriguing that glutamate dehydrogenase 1 (GLUD 1) and the related glutamate dehydrogenase 2 (GLUD 2) are up-regulated in the liver of MMA patients studied here (Figure 3). Perhaps the targeted inhibition of these enzymes, with concomitant

anaplerotic therapy directed toward the Krebs cycle, might present a new therapeutic approach to the treatment of hyperammonemia in MMA.

Some of the differentially regulated enzymes we have noted, while lacking direct and obvious connections to MMA, have also been seen in other forms of liver disease with steatosis and mitochondrial dysfunction[28]. For example, in the study of ethanol induced liver disease in rats, aldehyde dehydrogenase (ALDH2), carbonic anhydrase I (CA I), and glutamate dehydrogenase 1 (GLUD1) were differentially upregulated in the disease state, to a similar magnitude as we have observed in the MMA patient livers. Whether this represents a common response to hepatic injury or commonality in underlying pathophysiology is uncertain, but might be investigated in future experiments by determining the sensitivity of MMA mouse models to ethanol and assessing ethanol sensitivity in the patients for untoward toxicity.

We are cognizant that metabolism differs between cell types, and studied liver extracts because of the relevance of the liver to MMA and the relative abundance of hepatocytes in the liver compared to the biliary tract and supportive cells, such as Kuppfer cells. Thus although we cannot definitively assign dysregulated proteins to distinct cell types within the liver, our study constitutes the initial step to explore the proteome in MMA. Likewise, we recognize that the lack of age and sex matched controls is not ideal but have been practically constrained by the availability of control human livers from such a population, and therefore have used livers that were available through a donor program and quality controlled by testing each sample for the ability to yield viable and normal appearing hepatocytes. Future studies should concentrate on using iPS-derived hepatocytes, perhaps with and without correction with the MUT gene, to further extend this work.

Conclusions

In summary, we have discovered that diminished or absent MUT activity caused changes of enzymes involved in energy metabolism, gluconeogenesis and Krebs cycle anaplerosis. The identification of proteins whose expression was altered by MUT deficiency, and their respective pathways, could represent useful targets for further research and perhaps as targets for new therapies designed to alleviate the symptoms of the disease.

Acknowledgements

RJC, JLS, and CPV were supported by the Intramural Research Program of the National Human Genome Research Institute, NIH. SS was supported by the the Torsten och Ragnar Söderberg Stiftelse. KD was supported by the NIGMS/NIH COBRE grant P20 GM103549. SS was supported by the the Torsten och Ragnar Söderberg Stiftelse and the Vetenskaprådet, the Swedish Research Council.

References

1. W.A. Fenton, R.A. Gravel and D.S. Rosenblatt. *The Metabolic and Molecular Bases of Inherited Disease*, 8th edn. McGraw-Hill: New York. In: Scriver, CR, Sly, WS, Childs, B, Beaudet AL, Valle, D, Kinzler, KW et al. (eds) (2001). pp. 2165–2192.
2. H.O. de Baulny, J. F. Benoist, O. Rigal, G. Touati, D. Rabier and J. M. Saudubray. *J Inherit Metab Dis* (2005). 28: 415–423.
3. S.B. Van der Meer, F. Poggi, M. Spada, J. P. Bonnefont, H. Ogier, P. Hubert, E. Depondt, D. Rapoport, D. Rabier, C. Charpentier, P. Parvy, P. Kamoun, and J. M. Saudubray. *J. Pediatr* (1994) 125: 903–908
4. N.S. Hauser, I. Manoli, J.C. Graf, J. Sloan and C.P .Venditti. *Am J Clin Nutr* (2011). 93(1): 47-56.
5. E.R. Baumgarter, and C. Viardot. *J. Inherit. Metab. Dis* (1995) 18: 138–142.
6. P. Nicolaides, J. Leonard and R. Surtees. *Arch. Dis. Child* (1998). 78: 508–512.
7. C. Dionisi-Vici, F. Deodato, W. Roschinger, W. Rhead and B. Wilcken. *J. Inherit. Metab. Dis.* (2006). 29: 383–389.
8. B. Korf, J.K. Wallman, and H.L. Levy. *Ann. Neurol* (1986). 20: 364–366.
9. R. Heidenreich, M. Natowicz, B.E. Hainline P. Berman, R.I. Kelley, R.E. Hillman and G.T. Berry. *J. Pediatr* (1988). 113: 1022–1027.
10. S.G. Kahler, W.G. Sherwood, D. Woolf, S.T. Lawless, A. Zaritsky, J. Bonham, C. J. Taylor, J.T. Clarke, P. Durie and J.V. Leonard. *J. Pediatr* (1994). 124: 239–243.
11. J.H. Walter, A. Michalski, W.M. Wilson, J.V. Leonard, T.M. Barratt and M.J. Dillon *Eur. J. Pediatr* (1989). 148: 344–348
12. P. Kaplan, C. Ficicioglu, A.T. Mazur, M.J. Palmieri and G.T. Berry. *Mol Genet Metab* (2006). 88: 322–326.

13. M. Kasahara, R. Horikawa, M. Tagawa, S. Uemoto, S. Yokoyama, Y. Shibata, T. Kawano, T. Kuroda, T. Honna, K. Tanaka, M. Saeki. *Pediatr Transplant* (2006). 10: 943–947.

14. D. Morioka, M. Kasahara, R. Horikawa, S. Yokoyama, A. Fukuda and A. Nakagawa. *Am J Transplant* (2007). 7: 2782–2787.

15. A. Brassier O. Boyer, V. Valayannopoulos, C. Ottolenghi, P. Krug, M.A. Cosson, G. Touati, J.B. Arnoux, V. Barbier, N. Bahi-Buisson, I. Desguerre, M. Charbit, J.F. Benoist, L. Dupic , Y. Aigrain, T. Blanc, R. Salomon, D. Rabier, G. Guest, P. de Lonlay and P. Niaudet. *Mol Genet Metab* (2013). 110: 106-10.

16. W.G. van't Hoff, M. Dixon, J. Taylor, P. Mistry, K. Rolles, L. Rees and J.V. Leonard . *J Pediatr* (1998). 132: 1043–1044.

17. S. Nagarajan, G.M. Enns, M.T. Millan, S. Winter, and M.M. Sarwal. *J Inherit Metab Dis* (2005). 28: 517–524.

18. R.J. Chandler, J.Sloan, H. Fu, M. Tsai, S. Stabler, R. Allen, K.H. Kaestner, H.H. Kazazian, C.P. Venditti. *BMC Med Genet* (2007).8: 64.

19. R.J. Chandler, P.M. Zerfas, S. Shanske, J. Sloan, V. Hoffmann, S. Di Mauro, C.P. Venditti. *FASEB J*. (2009). 23(4): 1252-61.

20. I. Manoli, J. Sysol, .L Li, P. Houillier, C. Wang, P. Zerfas, K. Cusmano-Ozog, S. Young, N.S. Trivedi, J. Cheng, J.L. Sloan, R.J. Chandler, M. Abu-Asab, M. Tsokos, A.G. Elkahlooun, S. Rosen, G.M. Enns, G.T. Berry, V. Hoffman, S. DiMauro, J. Schnermann and C.P. Venditti. *Proc Natl Acad Sci USA*. (2013). 110(33): 13552–13557.

21. F. Catanzano, D. Ombrone, C. Di Stefano, A. Rossi, N. Nosari, E. Scolamiero, I. Tandurella, G. Frisso, G. Parenti, M. Ruoppolo, G. Andria and F. Salvatore. *J Inherit Metab Dis* (2010). 33: S91-4.

22. M. Caterino, C. Corbo, E. Imperlini, M. Armiraglio, E. Pavesi, A. Aspesi, F. Loreni, I. Dianzani and M. Ruoppolo. *Proteomics*. (2013) 13(7): 1220-7.

23. M. Caterino, A. Pastore, M. G Strozziero, G. Di Giovamberardino, E. Imperlini, E. Scolamiero, L. Ingenito, S. Boenzi, F. Ceravolo, D. Martinelli, C. Dionisi-Vici, M. Ruoppolo. *J Inherit Metab Dis* (2015). 38(5):969-79.

24. E. Imperlini, S. Orrù, C. Corbo, A. Daniele and F. Salvatore. Altered brain protein expression profiles are associated with molecular neurological dysfunction in the PKU mouse model. *J Neurochem*. (2014). 129(6):1002-12.

25. Y. Wilnai, G.M. Enns, A.K. Niemi, J. Higgins, H. Vogel. *Ultrastruct Pathol*. (2014) 38(5): 309-14

26. M.A. Schwab, S.W. Sauer, J.G. Okun, L.G. Nijtmans, R.J. Rodenburg, L.P. van den Heuvel, S. Dröse, U. Brandt, G.F. Hoffmann, H. Ter Laak, S. Kölker, J.A. Smeitink. *Biochem J.* (2006). 398: 107-12.

27. H.R. Filipowicz, S.L. Ernst, C.L. Ashurst, M. Pasquali, N. Longo. *Mol Genet Metab*. (2006). 88(2):123-30.

28. H. Fernando, J.E. Wiktorowicz, K.V. Soman , B.S. Kaphalia, M.F. Khan, G. A. Shakeel Ansari. *Toxicol Appl Pharmacol.* (2013). 266(3):470-80.

Figure Legends

Figure 1: Preparative 2D gel carried out using 24cm pH 3-10 NL in the first dimension and 10% SDS PAGE in the second dimension. The differentially expressed spots, picked-out and used for subsequent identification by mass spectrometry are labeled with official symbols reported in Tables 3 and 4.

Figure 2: A) Western Blot analysis of protein lysates using livers from controls and MMA patients. Proteins were separated on 10% SDS-PAGE and immunoblotted with specific antibodies **B)** Densitometric measurements of Western Blot analysis of protein lysates using livers from controls and MMA patients. The results are shown as mean ± SD (three replicates).

Figure 3: Metabolic pathways. Proteins marked with ↓ were found downregulated, proteins marked with ↑ were found up regulated.

Supplemental figures

Figure 1S: Picture of DIGE analytical gels images for the six replicates analysed. The overlay images of Cy3-Cy5-Cy2 images are shown.

Figure 2S: IPA output: A) The highest scoring Network Carbohydrate Metabolism, Score 41 has been obtained from the 56 identified proteins. Solid lines = direct interactions between two nodes; dashed lines = indirect interactions between two nodes. Arrowheads indicate directionality of the relationship. The various shapes of nodes denote the different functions

(legend). B) List of proteins constituting nodes in network shown in A. Proteins shown in bold have been identified in this study. Arrows indicate disregulation identified in this study.

Table 1. Characterization of the MMA patients (M1-M6) and control livers (C1-C6)

	Age transplant (months) *	Sex	Clinical features	Mutation 1	Mutation 2	Organs transplanted
M1	5	M	B12 non-responsive	c.670G>T p.E224X	c.682C>T p.E228X	LK
M2	24	M	B12 non-responsive	c.572C>A p.A191E	c.682C>T p.E228X	LK
M3	11	M	B12 non-responsive	c.682C>T p.E228X	c.1332+1delG p.splice	LK
M4	3	F	B12 non-responsive	c.682C>T p.E228X	c.1106G>A p.R369H	L
M5	15	F	B12 non-responsive	n/a	n/a	LK
M6	17	F	B12 non-responsive	n/a	n/a	LK
C1		M	ICH: donor, hx of 4x bypass, IDDM			
C2		F	SAH: donor			
C3		M	Head trauma/ MVA: donor			
C4		M	CVA: donor, hx of HTN and IDDM			
C5		M	ICH: donor			
C6		F	Anoxia/ICH: Non heart beating donor			

* The ages and mutation status, when determined, are presented.

ICH intracranial hemorrhage

IDDM insulin dependent diabetes mellitus

SAH subarachnoid hemorrhage

MVA motor vehicle accident

HTN hypertension

CVA cerebrovascular accident

L Liver, K Kidney

Table 2. Metabolites quantization using liver tissues from controls and MMA patients.

Metabolite						
	MMA patients					
	M1	**M2**	**M3**	**M4**	**M5**	**M6**
C3 propionylcarnitine (nM/ug of proteins)	50.2 ± 3,.0	12.5 ± 1.95	36.6 ± 5.1	66.0 ± 5.1	70.3 ± 1.79	66.8 ± 4.86
C4DC methylmalonylcarnitine (nM/ug of proteins)	3.51 ± 0.70	3.89 ± 0.59	5.40 ± 1.06	2.3 ± 0.33	2.7 ± 0.42	1.9 ± 0.32
C0 free carnitine (nM/ug of proteins)	235.8 ± 4.0	215.6 ± 13.4	261.2 ± 40.1	296.7 ± 48.8	221.1 ± 9.02	180.8 ± 14.4
Glycine (nM/ug of proteins)	0.56 ± 0.05	1.10 ± 0.04	0.69 ± 0.07	0.65 ± 0.06	0.21 ± 0.01	0.10 ± 0.01
Methylmalonic acid (µM/µg of proteins)	0.65 ± 0.17	0.72 ± 0.28	1.15 ± 0.07	0.52 ± 0.07	0.97 ± 0.14	0.87 ± 0.14
Succinate (µM/µg of proteins)	0.66 ± 0.20	0.49 ± 0.02	0.47 ± 0.02	0.57 ± 0.02	0.53 ± 0.10	0.40 ± 0.03
	Controls					
	C1	**C2**	**C3**	**C4**	**C5**	**C6**
C3 propionylcarnitine (nM/ug of proteins)	1.29 ± 0.09	0.10 ± 0. 3	0.60 ± 0.21	1.86 ± 0.57	1.92 ± 0.18	0.83 ± 0.24
C4DC methylmalonylcarnitine (nM/ug of proteins)	0.25 ± 0.03	0.14 ± 0.02	1.12 ± 0.12	0.14 ± 0.05	0.08 ± 0.04	0.072 ± 0.03
C0 free carnitine (nM/ug of proteins)	41.5 ± 1.5	39.8 ± 3.5	80.3 ± 3.4	23.7 ± 5.4	31.9 ± 3.8	33.0 ± 4.6
Glycine (nM/ug of proteins)	0.20 ± 0.02	0.22 ±0.02	0.41 ± 0.03	0.35 ± 0.04	0.30 ± 0.02	0.18 ± 0.02
Methylmalonic acid (µM/µg of proteins)	nd	nd	nd	nd	nd	nd
Succinate (µM/µg of proteins)	2.71 ± 0.16	3.26 ± 0.75	8.83 ± 0.64	5.50 ± 0.71	3.04 ± 0.51	4.21 ± 0.44

Table 3. Up-regulated proteins

Fold change	p-value	n Spot	Preotein description	GI[(a)]	Gene ID	Official Symbol[(b)]	MW (kDa)	pI
(+) 1.98	0.008	1063	ALDH2 aldehyde dehydrogenase 2 family (mitochondrial)	119618380	217	*ALDH2*	56.4	6.63
(+) 1.75	0.001	1266	HMGCS2 3-hydroxy-3-methylglutaryl-CoA synthase 2 (mitochondrial)	260656028	3158	*HMGCS2*	56.6	8.40
(+) 1.73	0.004	1072	GLUD1 glutamate dehydrogenase 1	4885281	2746	*GLUD1*	61.4	7.66
(+) 1.69	0.006	1043	GLUD2 glutamate dehydrogenase 2	31377775	2747	*GLUD2*	61.4	8.63
(+) 1.69	0.006	1043	PHGDH phosphoglycerate dehydrogenase	23308577	26227	*PHGDH*	56.6	6.29
(+) 1.58	0.007	581	TF transferrin	37747855	7018	*TF*	77.1	6.81
(+) 1.53	0.006	1067	SELENBP1 selenium binding protein 1	1374792	8991	*SELENBP1*	52.4	5.93
(+) 1.52	0.017	1233	GPT glutamic-pyruvate transaminase (alanine aminotransferase)	119602483	2875	*GPT*	54.6	6.77
(+) 1.52	0.011	2470	CA1 carbonic anhydrase I	4502517	759	*CA1*	28.9	6.59
(+) 1.52	0.013	2185	ETFA electron-transfer-flavoprotein, alpha polypeptide	4503607	2108	*ETFA*	35.1	8.62
(+) 1.52	0.013	2185	GNB2L1 guanine nucleotide binding protein (G protein), beta polypeptide 2-like 1	62896535	10399	*GNB2L1*	35.1	7.60
(+) 1.50	0.013	888	HSPD1 heat shock 60kDa protein 1 (chaperonin)	31542947	3329	*HSPD1*	61.0	5.70
(+) 1.33	0,009	2007	SULT2A1 sulfotransferase family, cytosolic, 2A, dehydroepiandrosterone (DHEA)-preferring, member 1	29540545	6822	*SULT2A1*	33.8	5.69
(+) 1.32	0.008	2488	ECHDC2 enoyl CoA hydratase domain containing 2	28278545	55268	*ECHDC2*	31.1	9.03
(+) 1.31	0.006	2951	PEBP1 phosphatidylethanolamine binding protein 1	4505621	5037	*PEBP1*	21.0	7.01
(+) 1.28	0.011	1051	ALDH1B1 aldehyde dehydrogenase 1 family, member B1	25777730	219	*ALDH1B1*	57.2	6.36
(+) 1.24	0.004	2174	ECH1 enoyl CoA hydratase 1, peroxisomal	16924265	1891	*ECH1*	35.8	8.16
(+) 1.10	0,038	1086	UGP2 UDP-glucose pyrophosphorylase 2	62702281	7360	*UGP2*	56.9	8.15

(+) indicates that the protein is more abundant in MMA liver than in control liver
(a) sequence identification number provided by NCBI
(b) sequence identification number provided by HGNC

Table 4. Down-regulated proteins

Fold change	p-value	n Spot	Preotein description	GI[(a)]	Gene ID	Official Symbol[(b)]	MW (kDa)	pI
(-) 3.35	0.0005	2536	NNMT nicotinamide N-methyltransferase	5453790	4837	*NNMT*	29.6	5.56
(-) 2.34	0.030	3321	HP haptoglobin	306882	3240	*HP*	45.2	6.13
(-) 2.32	0.010	239	EEF2 eukaryotic translation elongation factor 2	4503483	1938	*EEF2*	65.4	6.41
(-) 2.11	0.080	2668	KRT10 keratin 10	21961605	3858	*KRT10*	58.8	5.13
(-) 1.97	0.006	1023	KRT8 keratin 8	62913980	3856	*KRT8*	53.7	5.52
(-) 1.91	0.020	1750	ALDOB aldolase B, fructose-bisphosphate	2160383	229	*ALDOB*	39.5	8.01
(-) 1.85	0.010	661	CCDC22 coiled-coil domain containing 22	7661844	28952	*CCDC22*	70.8	6.30
(-) 1.84	0.002	470	MSN moesin	119625804	4478	*MSN*	67.8	6.08
(-) 1.80	0.008	555	HSPA5 heat shock 70kDa protein 5 (glucose-regulated protein, 78kDa)	6470150	3309	*HSPA5*	72.3	5.07
(-) 1.73	0.004	1494	ASS1 argininosuccinate synthase 1	119608340	445	*ASS1*	46.5	8.08
(-) 1.53	0.001	879	PCK2 phosphoenolpyruvate carboxykinase 2 (mitochondrial)	2661752	5106	*PCK2*	70.7	7.57
(-) 1.52	0.007	851	ALDH4A1 aldehyde dehydrogenase 4 family, member A1	14043187	8659	*ALDH4A1*	61.7	8.25
(-) 1.52	0.007	851	CES1 carboxylesterase 1	1335304	1066	*CES1*	62.5	6.15
(-) 1.52	0.007	851	CFB complement factor B	14124934	629	*CFB*	85.5	6.67
(-) 1.52	0.007	633	HSPA1B heat shock 70kDa protein 1B	167466173	3304	*HSPA1B*	70.0	5.47
(-) 1.46	0.009	2476	CTSD cathepsin D	4503143	1509	*CTSD*	44.5	6.10
(-) 1.43	0.007	528	CPS1 carbamoyl-phosphate synthase 1, mitochondrial	56378231	1373	*CPS1*	164.9	6.30
(-) 1.40	0.004	2681	TPI1 triosephosphate isomerase 1	4507645	7167	*TPI1*	30.8	5.65
(-)1.36	0,01	1247	FGG fibrinogen gamma chain	70906437	2266	*FGG*	51.5	5.37
(-)1.36	0,01	1247	SYNCRIP synaptotagmin binding, cytoplasmic RNA interacting protein	15809588	10492	*SYNCRIP*	69.6	8.68
(-)1.36	0,01	1247	HSPD1 heat shock 60kDa protein 1 (chaperonin)	77702086	3329	*HSPD1*	61.0	5.70
(-)1.36	0,01	1247	PSMC2 proteasome (prosome, macropain 26S subunit, ATPase, 2	76879893	5701	*PSMC2*	48.6	5.71
(-) 1.35	0.010	629	UROC1 urocanase domain containing 1	21389467	131669	*UROC1*	74.8	6.34
(-) 1.34	0,002	628	PCCA propionyl CoA carboxylase, alpha polypeptide	65506442	5095	*PCCA*	80.1	7.24
(-) 1.32	0.009	1132	ATP5B ATP synthase, H+ transporting, mitochondrila F1 complex, beta polypeptide	89574029	506	*ATP5B*	56.6	5.26
(-) 1.31	0,02	148	ALDH1L1 aldehyde dehydrogenase 1 family, member L1	21614513	10840	*ALDH1L1*	98.8	5.63
(-) 1.29	0,006	266	NAA15 N(alpha) -acetyltransferase 15, NatA auxiliary subunit	27370703	80155	*NAA15*	101.3	7.23
(-) 1.29	0,02	882	EPHX2 epoxide hydrolase 2, cytoplasmic	10197682	2053	*EPHX2*	62.6	5.91
(-) 1.26	0,01	1795	GALE UDP-galactose-4-epimerase	119615489	2582	*GALE*	38.3	6.26
(-) 1.25	0,01	2167	NIT2 nitrilase family, member 2	9910460	56954	*NIT2*	30.6	6.83
(-) 1.23	0.030	2122	TST thiosulfate sulfurtransferase (rhodanese)	17402865	7263	*TST*	33.4	6.77
(-) 1.21	0,007	557	SDHA succinate dehydrogenase complex, subunit A flavoprotein	194381536	6389	*SDHA*	72.7	7.06
(-) 1.21	0,009	1802	AKR1A1 aldo-keto reductase family 1, member A1 (aldehyde reductase	119627378	10327	*AKR1A1*	36.6	6.32
(-) 1.16	0,02	2653	PRDX6 peroxiredoxin 6	4758638	9588	*PRDX6*	25.0	6.00
(-) 1.14	0,04	929	FTCD formiminotransferase cyclodeaminase	119629716	10841	*FTCD*	58.9	5.56
(-) 1.12	0,009	284	PYGL phosphorylase, glycogen, liver	3170407	5836	*PYGL*	97.1	6.71

(-) indicates that the protein is more abundant in control liver than in MMA liver
(a) sequence identification number provided by NCBI
(b) sequence identification number provided by HGNC

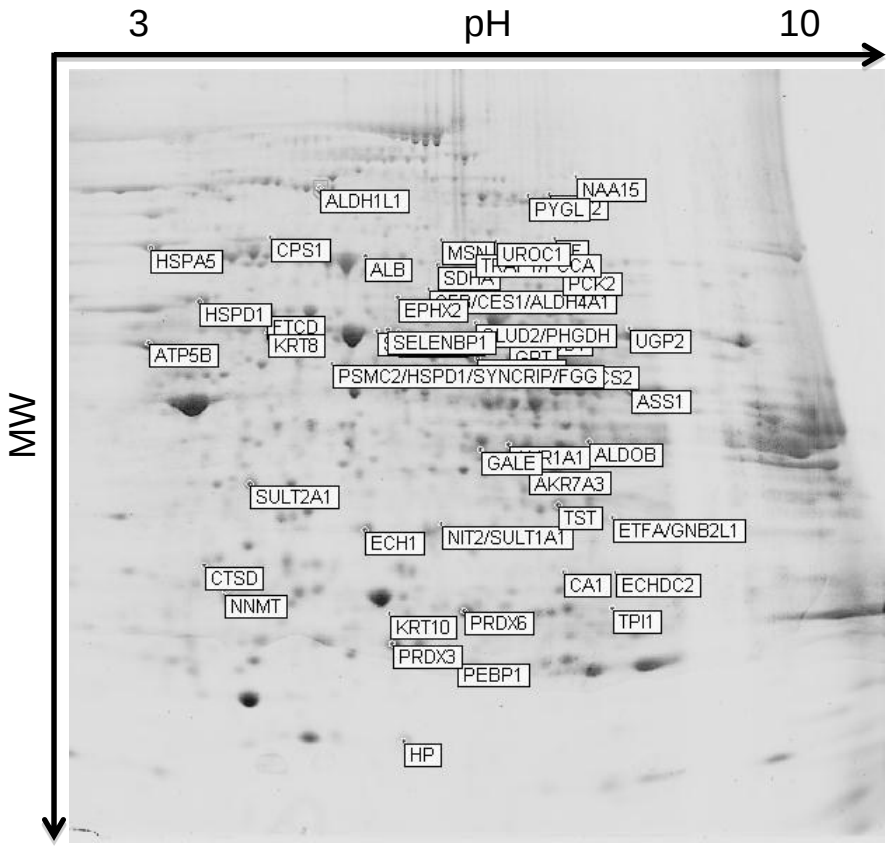

Figure 1

A

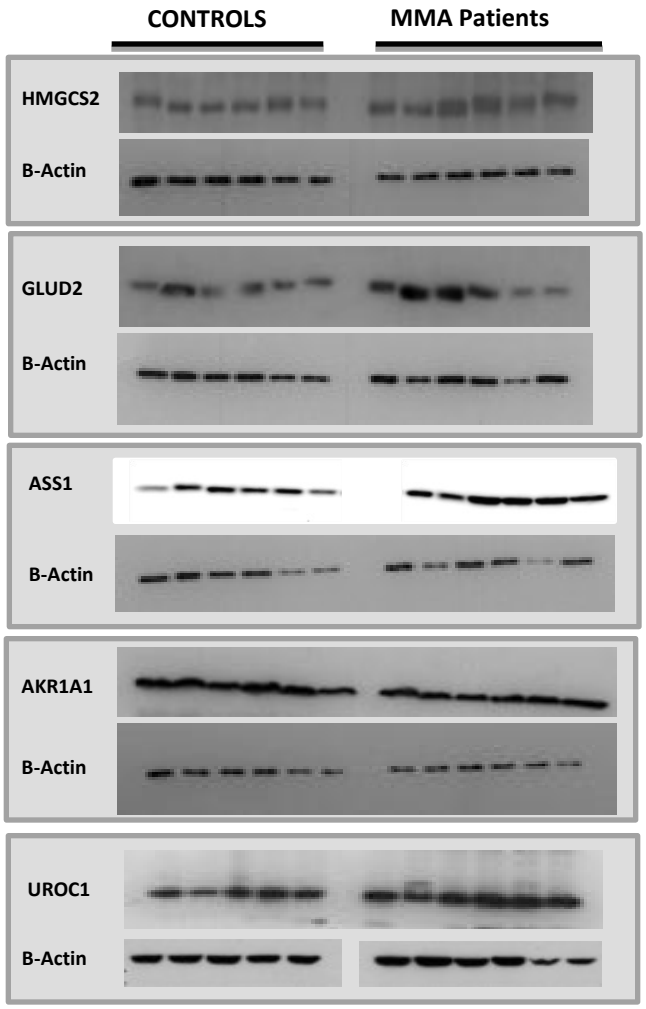

Figure 2

B

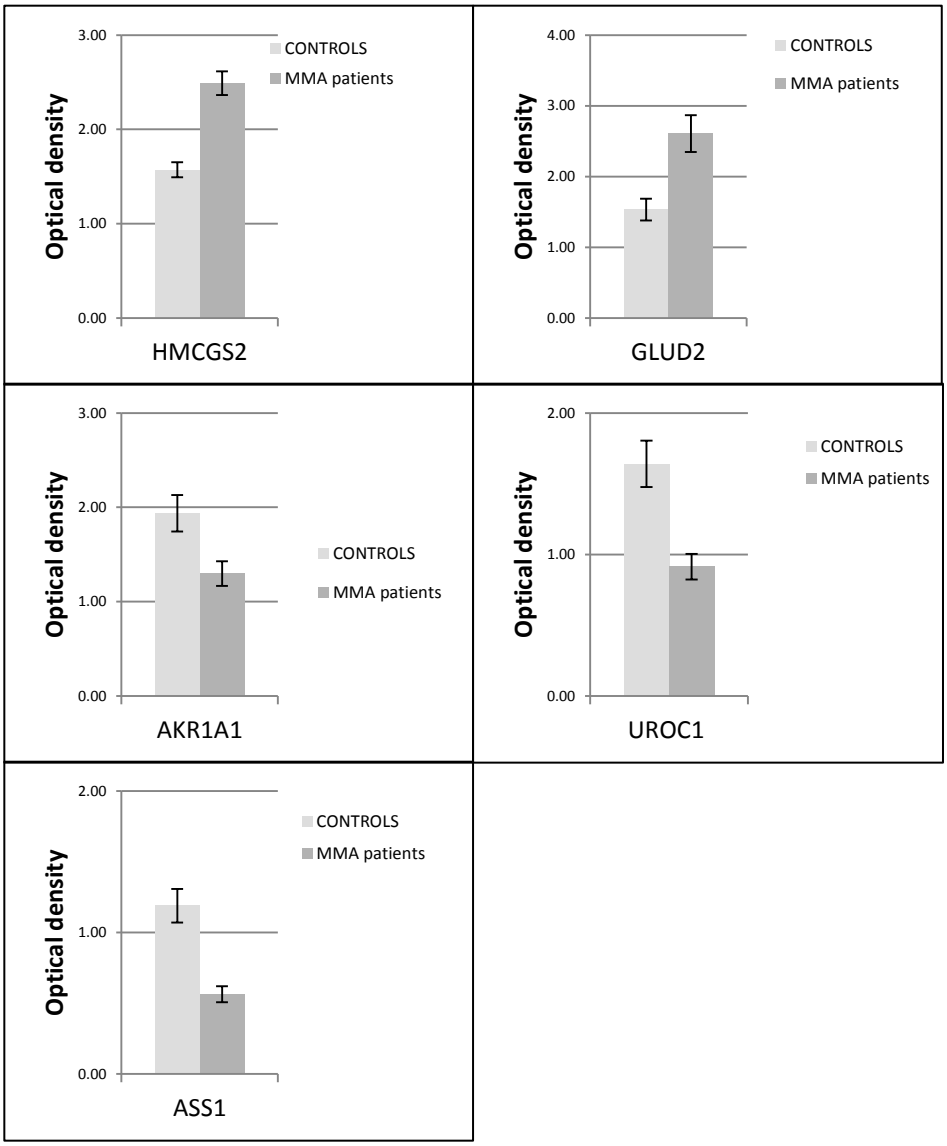

Figure 2

Figure 3